

See discussions, stats, and author profiles for this publication at: <https://www.researchgate.net/publication/236096364>

Steric Effects in the Reductive Coupling of CO by Mixed-Sandwich Uranium(III) Complexes

ARTICLE *in* ORGANOMETALLICS · MARCH 2013

Impact Factor: 4.13 · DOI: 10.1021/om301045k

CITATIONS

16

READS

31

4 AUTHORS, INCLUDING:



[Nikolaos Tsoureas](#)

University of Sussex

28 PUBLICATIONS 833 CITATIONS

SEE PROFILE



[Owen Summerscales](#)

Los Alamos National Laboratory

28 PUBLICATIONS 576 CITATIONS

SEE PROFILE



[Stephen Mark Roe](#)

University of Sussex

102 PUBLICATIONS 9,683 CITATIONS

SEE PROFILE

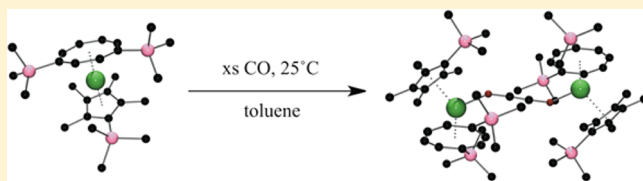
Steric Effects in the Reductive Coupling of CO by Mixed-Sandwich Uranium(III) Complexes

Nikolaos Tsoureas, Owen T. Summerscales, F. Geoffrey N. Cloke,* and S. Mark Roe

Division of Chemistry, School of Life Sciences, University of Sussex, Brighton BN1 9QJ, United Kingdom

Supporting Information

ABSTRACT: The selectivity of the mixed-sandwich U(III) complexes of the type $[\text{U}(\eta\text{-C}_8\text{H}_6\{\text{Si}^i\text{Pr}_3\text{-1,4}\}_2)(\eta\text{-Cp}^{\text{R}'})]$ ($\text{R} = \text{Me}$, ^iPr ; $\text{R}' = \text{Me}_4\text{H}$, Me_5 , Me_4^iPr , Me_4SiMe_3 , Me_4Et) toward the reductive coupling of CO to form uranium-bound oxocarbons has been explored. In this context, the new U(III) mixed-sandwich complexes $[\text{U}(\eta\text{-C}_8\text{H}_6\{\text{Si}^i\text{Pr}_3\text{-1,4}\}_2)(\eta\text{-Cp}^{\text{Me}_4\text{TMS}})]$, $[\text{U}(\eta\text{-C}_8\text{H}_6\{\text{Si}^i\text{Pr}_3\text{-1,4}\}_2)(\eta\text{-Cp}^{\text{Me}_4^i\text{Pr}})]$, $[\text{U}(\eta\text{-C}_8\text{H}_6\{\text{Si}^i\text{Pr}_3\text{-1,4}\}_2)(\eta\text{-Cp}^{\text{Me}_4\text{Et}})]$, $[\text{U}(\eta\text{-C}_8\text{H}_6\{\text{SiMe}_3\text{-1,4}\}_2)(\eta\text{-Cp}^*)]$, and $[\text{U}(\eta\text{-C}_8\text{H}_6\{\text{SiMe}_3\text{-1,4}\}_2)(\eta\text{-Cp}^{\text{Me}_4\text{TMS}})]$ have been prepared and structurally characterized. The reactivity toward CO is dominated by the “global” sterics around the uranium center, while selectivity for oxocarbon formation is largely regulated by the steric bulk of the $\text{Cp}^{\text{R}'}$ ligand. Accordingly, with excess CO $[\text{U}(\eta\text{-C}_8\text{H}_6\{\text{Si}^i\text{Pr}_3\text{-1,4}\}_2)(\eta\text{-Cp}^{\text{Me}_4\text{TMS}})]$ and $[\text{U}(\eta\text{-C}_8\text{H}_6\{\text{Si}^i\text{Pr}_3\text{-1,4}\}_2)(\eta\text{-Cp}^{\text{Me}_4^i\text{Pr}})]$ show no reactivity, $[\text{U}(\eta\text{-C}_8\text{H}_6\{\text{SiMe}_3\text{-1,4}\}_2)(\eta\text{-Cp}^{\text{Me}_4\text{TMS}})]$ is completely selective for the formation of the ynediolate complex $[\text{U}(\eta\text{-C}_8\text{H}_6\{\text{SiMe}_3\text{-1,4}\}_2)(\eta\text{-Cp}^{\text{Me}_4\text{TMS}})]_2(\mu\text{-}\eta^1\text{-}\eta^{1,13}\text{C}_2\text{O}_2)$, $[\text{U}(\eta\text{-C}_8\text{H}_6\{\text{Si}^i\text{Pr}_3\text{-1,4}\}_2)(\eta\text{-Cp}^*)]$ affords only the deltate complex $[\text{U}(\eta\text{-C}_8\text{H}_6\{\text{Si}^i\text{Pr}_3\text{-1,4}\}_2)(\eta\text{-Cp}^*)]_2(\mu\text{-}\eta^2\text{-}\eta^2\text{-C}_3\text{O}_3)$, and $[\text{U}(\eta\text{-C}_8\text{H}_6\{\text{Si}^i\text{Pr}_3\text{-1,4}\}_2)(\eta\text{-Cp}^{\text{Me}_4\text{H}})]$ gives solely the squarate complex $[\text{U}(\eta\text{-C}_8\text{H}_6\{\text{Si}^i\text{Pr}_3\text{-1,4}\}_2)(\eta\text{-Cp}^{\text{Me}_4\text{H}})]_2(\mu\text{-}\eta^2\text{-}\eta^2\text{-C}_4\text{O}_4)$. Additionally, the squarate moiety has been removed from the uranium center in the last complex by reaction with Me_3SiCl to afford the TMS ester of squaric acid, $\text{C}_4\text{O}_2(\text{OTMS})_2$.



INTRODUCTION

The activation of small molecules by well-defined molecular species offers energy- and atom-efficient as well as environmentally friendly new routes for their chemical transformations.¹ Within this framework, organometallic complexes of uranium have attracted significant interest over the past few years,² with examples including the reductive activation of N_2 ,³ CO_2 ,⁴ NO ,⁵ and CO .⁶ The last species is of significant importance, as it can be derived from CO_2 , utilizing the water-gas shift reaction,⁷ and plays an important role in many catalytic and atom-efficient reactions such as the hydroformylation of olefins.⁸ In this context the reductive coupling of $n\text{CO}$ ($n = 2\text{--}6$) molecules to furnish the series of linear ($n = 2$) and cyclic oxocarbon dianions ($n = 3\text{--}6$) (Figure 1) is the archetypical atom-efficient reaction. Previous reports of their direct synthesis from CO involves molten alkali metals,^{9a,b} overpressures of CO ,^{9a-c} and, in certain cases, electrochemical setups.^{9d,e}

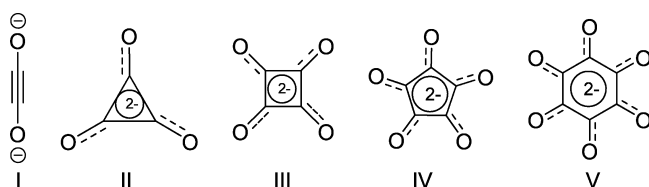


Figure 1. The oxocarbons: I, ynediolate; II, deltate; III, squarate; IV, croconate; V, rhodizionate.

In 2006 our group reported an alternative route to accessing these oxocarbons, under very mild conditions, using the U(III) mixed-sandwich organometallic complex **1** to produce dimer **4**, where two U(IV) centers are bridged by the deltate dianion (Scheme 1).¹⁰ Furthermore, it was found that careful manipulation of the ligand environment or the stoichiometry of the added CO can significantly alter the reaction products to furnish the squarate dimer **5**¹¹ or the ynediolate dimer **3**,¹² respectively (Scheme 1). A theoretical study has suggested that the formation of the ynediolate dimer **3** is the kinetic product of the reductive coupling of CO, while the higher cyclic oxocarbon dimers, e.g. the deltate **4**, are the thermodynamically favored products of the reaction.¹³ Since then, other groups¹⁴ have established the efficiency of U(III) complexes in the reductive coupling of CO and have demonstrated the potential of this transformation to yield substituted furans, with recycling of the U(III) complex, albeit not catalytically.¹⁵

The scope of using U(III) complexes for the derivatization of CO was further exemplified by the isolation of the $\text{U}^{\text{IV}}\text{--OMe}$ complex $[\text{U}(\eta\text{-C}_8\text{H}_6\{\text{Si}^i\text{Pr}_3\text{-1,4}\}_2)(\eta\text{-Cp}^*)\text{OMe}]$ (**6**), formed by reaction of complex **1** with stoichiometric syngas (Figure 2).¹⁶ It was also shown that the methoxide moiety can be extruded in the form of SiMe_3OMe , using SiMe_3OTf ($\text{OTf} = \text{CF}_3\text{SO}_3$), and the resulting $\text{U}^{\text{IV}}\text{--OTf}$ complex can be reduced back to the U(III) complex **1** with KC_8 (Figure 2).¹⁶

Special Issue: Recent Advances in Organo-f-Element Chemistry

Received: November 2, 2012

Published: December 14, 2012

Scheme 1. Synthesis of Different Size Oxocarbons by Manipulation of Steric Environment and Stoichiometry

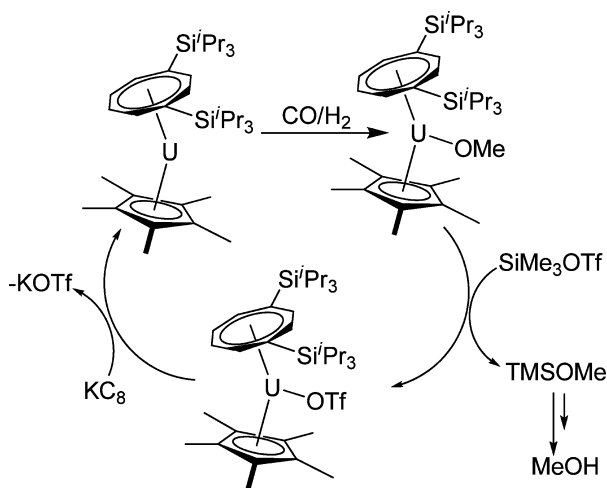
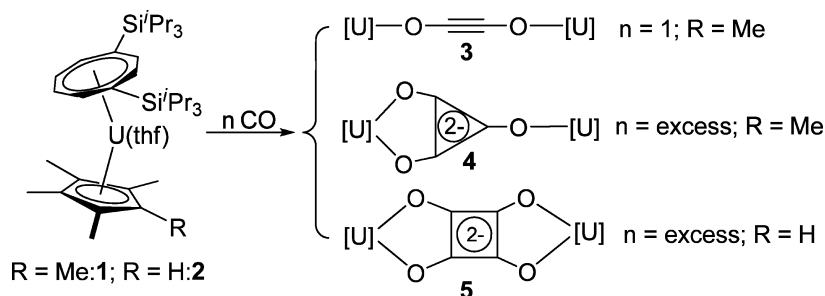


Figure 2. Formation of MeOH by reductive coupling of syngas on a U(III) metal center and stoichiometric recycling of the U(III) starting material.

One drawback of this system is the propensity of complex **1** to react with any excess of CO to yield the deltate complex **4**¹¹ (Scheme 1), effectively completely retarding the formation of **6** unless the stoichiometry is carefully controlled. Hence, as well as further elaborating the selectivity of oxocarbon formation by this system in general, we were particularly interested in exploring whether *selective* formation of the ynediolate dimers of type **3** (and hence possibly methoxides of type (**6**)) with an *excess* of CO could be achieved via manipulation of the steric environment around the uranium center.

EXPERIMENTAL SECTION

General Considerations. All manipulations were carried out in a MBraun glovebox under N₂ or Ar (O₂ and H₂O <1 ppm) or by using standard Schlenk techniques under Ar (BOC pureshield) passed through a column containing BASF R3-11(G) catalyst and activated molecular sieves (4 Å). All glassware was dried at 160 °C overnight prior to use. Celite was predried in a 200 °C oven and then heated at 230 °C overnight under dynamic vacuum (2 × 10⁻² mbar) and stored in a glovebox under Ar prior to use. Filter cannulas were prepared using Whatman 25 mm glass microfiber filters and were predried at 160 °C overnight. THF and toluene were dried over molten K and distilled under a N₂ atmosphere and were kept in Young ampules over activated molecular sieves (4 Å) or a potassium mirror, respectively, under Ar. Hydrocarbons (*n*-pentane, *n*-hexane) and Et₂O were dried over NaK, distilled under a N₂ atmosphere, and kept in Young ampules over a potassium mirror under Ar. Deuterated toluene, pyridine, cyclohexane, benzene, and THF were degassed by three freeze–thaw cycles, dried by refluxing over K for 3 days, vacuum-distilled, and kept in a flame-dried Young ampule in the glovebox under N₂. K[N(SiMe₃)₂] was purchased from Aldrich and was

recrystallized from toluene prior to use. Cp^{Me⁴Et}H was purchased from Aldrich and used as received. ¹³CO (99.7% enrichment) gas was purchased from EuroIsotop and was transferred via an accurately calibrated Toepler pump. ¹²CO was research grade (99.997%) and was purchased from BOC. Cp^{Me⁴Pr}H was prepared via a method analogous to that reported for Cp^{Me⁴Bu}H¹⁷ using ⁱPrLi (see below). The following materials were prepared according to literature methods: UI₃,¹⁸ UCp*₂(THF)₃,¹⁹ Cp^{Me⁴TMS}H,²⁰ K₂[C₈H₆{SiPr₃-1,4}₂] (referred to as K₂COT^{tip}s²), K₂[C₈H₆{SiMe₃-1,4}₂]²¹ (referred to as K₂COT^{tms}s²), KCH₂Ph,²² [U(η-C₈H₆{SiPr₃-1,4}₂)(η-Cp^{Me⁴H})₂(μ-η²:η²-C₄O₄)₂]¹¹ and [U(η-C₈H₆{SiPr₃-1,4}₂)(η-Cp*)₂(μ-η²:η²-C₃O₃)₂].¹⁰

¹H, ¹³C{¹H}, and ²⁹Si{¹H} NMR data were recorded on a Varian VNMR S400 spectrometer operating at 400 MHz (¹H). The spectra were referenced internally to the residual protic solvent (¹H) or the signals of the solvent (¹³C). ²⁹Si{¹H} NMR were referenced externally relative to SiMe₄. All spectra were recorded at 30 °C unless otherwise stated. EI-MS mass spectra were recorded on a VG-Autospec Fisons instrument at the University of Sussex. Elemental analyses were performed by Mikroanalytisches Labor Pascher. In situ IR measurements were carried out using a ReactIR system in a specially designed cell connected to the Toepler line.

Cp^{Me⁴Pr}H. A 2.76 g portion of 2,3,4,6-tetramethylcyclopent-2-enone (20 mmol) was degassed by two freeze–thaw cycles in a Young ampule, and dry Et₂O (40 mL) was added to it to produce a pale yellow solution. This solution was cooled to −78 °C, and 35 mL of a 0.6 M solution of ⁱPrLi in *n*-pentane (21 mmol) was added dropwise over 3 h. After the addition was complete, the reaction mixture was stirred overnight, upon which time the temperature of the slush bath had reached 10 °C. The slush bath was then removed and the solution stirred for another 3 days at room temperature. It was then cooled to 0 °C, and the excess ⁱPrLi was carefully quenched by dropwise addition of H₂O under Ar. After bubbling had ceased, a dusky brown solution had formed, which was stirred at room temperature for 1 h. It was then treated with vigorous stirring with 33% (v/v) of H₂SO₄ dropwise until the dusky brown solution disappeared to give a biphasic reaction mixture with a pink hue that was stirred at room temperature for 1 h. The two layers were separated, and the Et₂O layer was washed with 2 × 15 mL of the H₂SO₄ solution, 25 mL of H₂O, and finally with 25 mL portions of saturated Na₂CO₃(aq) until the aqueous washings had a pH of approximately 7. The combined water phase was then extracted with 30 mL of Et₂O, the organic layers were combined and dried over MgSO₄, and volatiles were removed in a rotary evaporator (at 50 mbar pressure). The residue was then distilled at 46–48 °C at 1 mmHg to yield 1.54 g (47% yield) of the title compound as a mixture of three isomers with purity >90% (as judged by GC-MS).

Note: the preparative procedure by Schumann et al.²³ reports an erroneous bp of 68 °C at 1 mmHg.

K⁺[Cp^{Me⁴Pr}][−]. A 500 mg portion of Cp^{Me⁴Pr}H (3.05 mmol) in a Young ampule was degassed by two freeze–thaw cycles, and dry THF (20 mL) was added to yield a pale yellow solution. This was cooled to 0 °C and treated dropwise with a solution of 398 mg (1 mol equiv) of potassium benzyl in THF (10 mL) over ca. 10 min. After the addition was complete, a white precipitate started forming almost instantly, and the reaction mixture was stirred for 2 days at room temperature. It was then filtered in the glovebox through a porosity 4 sintered-glass frit to

yield a white-orange precipitate, which subsequently was washed with THF until the washings were colorless and *n*-pentane (3 × 20 mL) and dried under vacuum to yield the title compound as a white powder. Yield: 400 mg (65%). The procedure can be scaled up 5-fold with no reduction in yield. $K^+[Cp^{Me_4TMS}Pr]^-$ is insoluble in THF.²⁴ ¹H NMR (δ C₅D₅N, 70 °C): 1.46 (d, ³J_{HH} = 7.01 Hz, 6H, CH(CH₃)₂), 2.26 (s, 6H, CH₃), 2.29 (s, 6H, CH₃), 3.29 (sept, ³J_{HH} = 7.01 Hz, 1H, CH(CH₃)₂).

$K^+[Cp^{Me_4TMS}Pr]^-$. A 2.74 g portion of Cp^{Me₄TMS}Pr (14.1 mmol) in a Young ampule was degassed by two freeze–thaw cycles, and dry toluene (8–10 mL) was added to yield a pale yellow solution. This was cooled to 0 °C and added dropwise to a solution of 2.8 g of K[N(SiMe₃)₂] (14.07 mmol, 0.99 mol equiv) in toluene (20 mL) over ca. 30 min. After the addition was complete, a white precipitate started forming almost instantly, and the reaction mixture was stirred overnight at 32 °C. It was then filtered in the glovebox through a porosity 4 sintered-glass frit to yield a white powder, which subsequently was washed with toluene (2 × 20 mL), and *n*-pentane (3 × 20 mL) and dried under vacuum to yield the title compound as a white powder. Yield: 3.0 g (91%) ¹H NMR (δ C₅D₅N, 50 °C): 0.35 (s, 3H, Si(CH₃)₃), 0.50 (s, 6H, Si(CH₃)₃), 2.34 (s, 6H, CH₃), 2.49 (s, 6H, CH₃).

General Method for the Preparation of Complexes [U(η -C₈H₆{SiⁱPr₃-1,4₂})(η -Cp^R)] (R = Me₄Et, Me₄TMS, Me₄Pr): Method A. In a typical procedure, to 1.23 g (1.99 mmol) of U₃ dissolved in THF (50 mL) in a Young ampule was added 1 mol equiv of the KCp^R salt suspended in THF (20 mL) dropwise via cannula to give a pine-green solution that was stirred overnight. Volatiles were then removed under vacuum. The dark green residue was extracted into toluene (2 × 30 mL), and the extract was filtered via cannula into a Young ampule. The resulting green solution was stripped off of volatiles under vacuum, and the residue was redissolved in THF (50 mL) and cooled to –45 °C. To this solution was added dropwise a THF solution of K₂COT^{tips2} (0.8–0.9 mol equiv) over 1½ h, and after completion of the addition the resulting reaction mixture was warmed to room temperature overnight to yield a brown-black solution with a white precipitate. Volatiles were removed under vacuum to furnish a brown residue that was extracted into *n*-pentane (60 mL), and the extract was filtered through Celite on a frit. The resultant dark brown solution was reduced in volume (approximately half), freeze–thawed (to ensure complete precipitation of KI), filtered via cannula, and either reduced in volume to ca. 30 mL and cooled to –45 °C to yield crystals of the title compound or stripped of volatiles and the residue recrystallized from the appropriate solvent (see procedure for individual complexes 7–9 below). The compounds were stored in the glovebox at –35 °C.

General Method for the Preparation of Complexes U(η -C₈H₆{SiMe₃-1,4₂})(η -Cp^R)(THF)_x (R = Me₅, Me₄TMS; x = 0, 1): Method B. The procedure was as per method A above, *except* that the final reaction mixture was left at room temperature for 1 h only. Leaving the reaction mixture, after completion of addition of K₂COT^{tips2}, at room temperature for prolonged periods of time results in reduced yields of the isolated complexes or even in no isolation of the title compounds, probably due to a disproportionation pathway leading to the formation of [U(η -C₈H₆{SiMe₃-1,4₂})₂]. The compounds are thermally unstable in the solid state, and decomposition occurs over ca. 2–3 days at room temperature, as evidenced by ¹H NMR spectroscopy. Accordingly they were stored in the glovebox at –35 °C.

[U(η -C₈H₆{SiⁱPr₃-1,4₂})(η -Cp^{Me₄Et})] (7). Prepared according to method A and recrystallized from *n*-hexane by slow evaporation at room temperature in the glovebox. Yield: 740 mg (49.5%). ¹H NMR (δ C₇D₈): –120.60 (br s, $\Delta\nu_{1/2}$ = 240.72 Hz, 2H, COT), –82.56 (br s, $\Delta\nu_{1/2}$ = 264.80 Hz, 2H, COT), –17.07 (s, 6H, CH₃), –15.62 (s, 6H, CH₃), –13.06 (s, 2H, Cp^{Me₄}-CH₂CH₃), –8.06 (s, 18H, COT-[Si{CH(CH₃)₂}]₂), –4.42 (s, 18H, COT-[Si{CH(CH₃)₂}]₂), –0.73 (s, 6H, COT-[Si{CH(CH₃)₂}]₂), 5.28 (s, 3H, Cp^{Me₄}-CH₂CH₃), 47.17 (br s, $\Delta\nu_{1/2}$ = 294.89 Hz, 2H, COT). ²⁹Si{¹H} NMR (δ C₇D₈): –136.65 (s, COT-[Si{CH(CH₃)₂}]₂). EI-MS: 822 (M + F), 803 (M), 673 (M – Cp^{Me₄Et} + F), 416 (COT^{tips2}), 373 (COT^{tips2} – ⁱPr), 157

([Si{CH(CH₃)₂}]₂). Anal. Calcd for C₃₇H₆₅Si₂U: C, 55.27; H, 8.15. Found: C, 55.15; H, 8.17.

[U(η -C₈H₆{SiⁱPr₃-1,4₂})(η -Cp^{Me₄Pr})] (8). Prepared according to method A and crystallized from (SiMe₃)₂O at –35 °C overnight to produce dark brown needles. Yield: 230 mg (18%, not optimized). ¹H NMR (δ C₇D₈): –116.83 (br s, $\Delta\nu_{1/2}$ = 235.59 Hz, 2H, COT), –79.00 (br s, $\Delta\nu_{1/2}$ = 205.52 Hz, 2H, COT), –29.03 (s, 6H, CH₃), –18.00 (s, 6H, CH₃), –13.79 (s, 1H, Cp^{Me₄}-CH(CH₃)₂), –6.83 (s, 18H, COT-[Si{CH(CH₃)₂}]₂), –3.89 (s, 6H, Cp^{Me₄}-CH(CH₃)₂), –3.21 (s, 18H, COT-[Si{CH(CH₃)₂}]₂), –0.18 (s, 6H, COT-[Si{CH(CH₃)₂}]₂), 40.61 (br s, $\Delta\nu_{1/2}$ = 230.58 Hz, 2H, COT). ²⁹Si{¹H} NMR (δ C₇D₈): –132.60 (s, COT-[Si{CH(CH₃)₂}]₂). EI-MS: 837 (M + F), 818 (M), 673 (M – Cp^{Me₄Pr} + F), 157 ([Si{CH(CH₃)₂}]₂). Anal. Calcd for C₃₈H₆₇Si₂U: C, 55.79; H, 8.25. Found: C, 55.24; H, 8.15.

[U(η -C₈H₆{SiⁱPr₃-1,4₂})(η -Cp^{Me₄TMS})] (9). Prepared according to method A and crystallized from *n*-hexane at –35 °C to produce large dark brown blocks. Yield: 450 mg (37.6% based on K₂COT^{tips2}). ¹H NMR (δ C₇D₈): –120.60 (br s, $\Delta\nu_{1/2}$ = 153.54 Hz, 2H, COT), –80.97 (br s, $\Delta\nu_{1/2}$ = 164.99 Hz, 2H, COT), –25.93 (s, 6H, CH₃), –22.62 (s, 9H, Cp^{Me₄}-Si(CH₃)₃), –6.36 (s, 18H, COT-[Si{CH(CH₃)₂}]₂), –2.72 (s, 6H, CH₃), –2.43 (s, 18H, COT-[Si{CH(CH₃)₂}]₂), 0.53 (s, 6H, COT-[Si{CH(CH₃)₂}]₂), 46.16 (br s, $\Delta\nu_{1/2}$ = 164.99 Hz, 2H, COT). ²⁹Si{¹H} NMR (δ C₇D₈): –123.60 (s, COT-[Si{CH(CH₃)₂}]₂), the signal of CpMe₄-SiMe₃ could not be located. EI-MS: 847 (M), 673 (M – Cp^{Me₄TMS} + F), 373 (COT^{tips2} – ⁱPr), 194 (Cp^{Me₄TMS}), 157 ([Si{CH(CH₃)₂}]₂). Anal. Calcd for C₃₈H₆₉Si₃U: C, 53.81; H, 8.20. Found: C, 53.54; H, 7.98.

[U(η -C₈H₆{SiMe₃-1,4₂})(η -Cp^{*})(THF)] (10a). Prepared according to Method B and crystallized from *n*-pentane at –45 °C overnight to furnish the title compound as black needles. Yield: 580 mg (52.5%). ¹H NMR (δ C₆D₆): –96.42 (br s, $\Delta\nu_{1/2}$ = 148.09 Hz, 2H, COT), –75.94 (br s, $\Delta\nu_{1/2}$ = 157.41 Hz, 2H, COT), –23.06 (s, 4H, CH₂ THF), –14.60 (s, 15H, Cp(CH₃)₃), –7.48 (s, 18H COT-{Si(CH₃)₃})₂, –4.86 (s, 4H, CH₂ THF), 22.70 (br s, $\Delta\nu_{1/2}$ = 146.02 Hz, 2H, COT). ²⁹Si{¹H} NMR (δ C₇D₈): –176.25 (s, COT-{Si(CH₃)₃})₂. EI-MS: 641 (M – THF + F), 621 (M – THF), 505 ([UCOT^{tips2}] + F), 486 ([UCOT^{tips2}]), 414 ([UCOT^{tips2}] – TMS), 135 (Cp^{*}). Elemental analysis on this compound could not be obtained due to its thermal instability.

Alternative Synthesis of [U(η -C₈H₆{SiMe₃-1,4₂})(η -Cp^{*})(THF)] (10a) from UCp^{*}I₂(THF)₃. A 650 mg portion of UCp^{*}I₂(THF)₃ (0.84 mmol) was placed in an ampule equipped with a greaseless stopcock and dissolved in approximately 50 mL of THF. This green solution was cooled to –45 °C and treated dropwise with a 30 mL solution of K₂COT^{tips2} (240 mg, 0.87 mol equiv) in THF over ca. 1½ h. After the addition was complete, the slush bath was removed and the green-brown reaction mixture was left to slowly equilibrate at room temperature over ca. 1 h. After removal of volatiles the workup described in method B was followed to furnish the title compound in an almost identical yield. Yield: 55%.

[U(η -C₈H₆{SiMe₃-1,4₂})(η -Cp^{*})] (10b). A 27 mg portion of [U(η -C₈H₆{SiMe₃-1,4₂})(η -Cp^{*})(THF)] (10a; 0.039 mmol) was placed in a preweighed Young NMR tube which was evacuated (10^{–6} mbar) at room temperature for 1 h, 55 °C for 1 h, 65 °C for another 1 h, and finally at 75 °C for 30 min to give a weight loss of 3.0 mg (calculated loss of all THF is 2.8 mg). The residue was then recrystallized from a minimum amount of toluene (approximately 0.5 mL) to give the title compound. Yield: 15 mg (62%). ¹H NMR (δ C₆D₁₂): –96.90 (br s, $\Delta\nu_{1/2}$ = 145.12 Hz, 2H, COT), –68.38 (br s, $\Delta\nu_{1/2}$ = 159.09 Hz, 2H, COT), –23.57 –14.60 (s, 15H, Cp(CH₃)₃), –10.02 (s, 18H COT-{Si(CH₃)₃})₂, 24.98 (br s, $\Delta\nu_{1/2}$ = 147.12 Hz, 2H, COT). ²⁹Si{¹H} NMR (δ C₆D₁₂): –145.26 (s, COT-{Si(CH₃)₃})₂. Satisfactory elemental analysis on this compound could not be obtained due to its thermal instability.

[U(η -C₈H₆{SiMe₃-1,4₂})(η -Cp^{Me₄TMS})] (11). Prepared according to method B and crystallized from *n*-hexane at –35 °C (two crops). Combined yield: 240 mg (22.2%). ¹H NMR (δ C₇D₈): –100.3 (br s, $\Delta\nu_{1/2}$ = 163.64 Hz, 2H, COT), –68.84 (br s, $\Delta\nu_{1/2}$ = 157.48 Hz, 2H, COT), –35.96 (s, 6H, CH₃), –28.61 (s, 9H, Cp^{Me₄}-Si(CH₃)₃), –8.00 (s, 18H, COT-{Si(CH₃)₃})₂, –4.67 (s, 6H, CH₃), 22.33 (br s, $\Delta\nu_{1/2}$ =

172.48 Hz, 2H, COT). $^{29}\text{Si}\{^1\text{H}\}$ NMR (δ C_7D_8): -154.13 (s, COT- $\{\text{Si}(\text{CH}_3)_3\}_2$), the signal of $\text{CpMe}_4\text{-SiMe}_3$ could not be located. EI-MS: 698 (M + F), 679 (M), 505 ($[\text{UCOT}^{\text{tms}2}] + \text{F}$), 486 ($[\text{UCOT}^{\text{tms}2}]$), 432 ($[\text{UCOT}^{\text{tms}2}] - \text{TMS} + \text{F}$), 414 ($[\text{UCOT}^{\text{tms}2}] - \text{TMS}$), 248 ($\text{COT}^{\text{tms}2}$), 73 (TMS). Satisfactory elemental analysis on this compound could not be obtained, due to its thermal instability.

[U(η -C₈H₆{SiⁱPr₃-1,4₂})(η -Cp^{Me₄Et})]₂(μ - η^1 - η^1 -¹³C₂O₂) (12). A 150 mg portion of $[\text{U}(\eta\text{-C}_8\text{H}_6\{\text{Si}^i\text{Pr}_3\text{-1,4}_2\})(\eta\text{-Cp}^{\text{Me}_4\text{Et}})]$ (0.187 mmol) was dissolved in 0.5–0.7 mL of *d*₈-toluene in a 50 mL ampule equipped with a Young valve which was attached to the Toepler line, and the solution was cooled to -78°C and then degassed by evacuating the headspace at this temperature. ¹³CO (3 mol equiv) was transferred, and the reaction mixture was warmed to room temperature overnight with stirring, after which time the solution had changed from brown to red. Volatiles were removed under vacuum, and the red residue was extracted into approximately 1–2 mL of *n*-pentane at room temperature and cooled to -35°C overnight, to afford crystals of the title compound; a further crop of product was obtained from the mother liquor by slow cooling to -78°C . Combined yield: 92 mg (59.1%). ¹H NMR (δ C_7D_8): -54.06 (s, 4H, COT), -33.13 (s, 4H, COT), -11.84 (br s, 12H, COT- $[\text{Si}\{\text{CH}(\text{CH}_3)_2\}_3]_2$), -9.51 (d, ³J_{HH} = 6.68 Hz, 36H, COT- $[\text{Si}\{\text{CH}(\text{CH}_3)_2\}_3]_2$), -3.26 (d, ³J_{HH} = 7.63 Hz, 36H, COT- $[\text{Si}\{\text{CH}(\text{CH}_3)_2\}_3]_2$), 1.91 (s, 12H, CH₃), 3.53 (s, 6H, Cp^{Me₄}-CH₂CH₃), 5.27 (s, 12H, CH₃), 5.84 (s, 4H, Cp^{Me₄}-CH₂CH₃), 55.25 (s, 4H, COT). ¹³C{¹H} NMR (δ C_7D_8): 315.46 (s, $[\text{U}]^{13}\text{C}_2\text{O}_2[\text{U}]$). ²⁹Si{¹H} NMR (δ C_7D_8): -112.54 (s, COT- $[\text{Si}\{\text{CH}(\text{CH}_3)_2\}_3]_2$). EI-MS: 1666 (M), 1534 (M – Cp^{Me₄Et} + F), 822 ($[\text{UCOT}^{\text{tms}2}\text{Cp}^{\text{Me}_4\text{Et}}] + \text{F}$), 803 ($\text{UCOT}^{\text{tms}2}\text{Cp}^{\text{Me}_4\text{Et}}$), 673 ($[\text{UCOT}^{\text{tms}2}] + \text{F}$). Anal. Calcd for C₇₆H₁₃₀O₂Si₄U₂: C, 54.90; H, 7.86. Found: C, 54.18; H, 7.82.

Reaction of [U(η -C₈H₆{SiⁱPr₃-1,4₂})(η -Cp^{Me₄Et})] (7) with 1.5 bar of CO. A Young NMR tube was charged in the glovebox with 16 mg of 7 (0.019 mmol), which was dissolved in 0.5 mL of C_7D_8 . The brown solution was freeze–thaw degassed, the tube was pressurized at either -78°C or room temperature with 1.5 bar (10 equiv) of CO, and the ¹H NMR spectra were recorded after 1 day at room temperature.

Reaction of [U(η -C₈H₆{SiⁱPr₃-1,4₂})(η -Cp^{Me₄Pr})] (8) with Excess/High Pressure CO. A Young NMR tube was charged in the glovebox with 20 mg of 8 (0.024 mmol) which was dissolved in 0.5 mL of C_7D_8 . The brown solution was freeze–thaw degassed, the tube was pressurized at either -78°C or room temperature with 1.5 bar (10 equiv) of CO, and the ¹H NMR spectra were recorded after 1 day at room temperature. ¹H NMR (δ C_7D_8): -105.37 (br s, $\Delta\nu_{1/2} = 343.55$ Hz, 2H, COT), -73.69 (br s, $\Delta\nu_{1/2} = 236.20$ Hz, 2H, COT), -26.17 (s, 6H, CH₃), -18.06 (s, 6H, CH₃), -13.79 (s, 1H, Cp^{Me₄}-CH(CH₃)₂), -6.24 (s, 18H, COT- $[\text{Si}\{\text{CH}(\text{CH}_3)_2\}_3]_2$), -4.80 (s, 6H, Cp^{Me₄}-CH(CH₃)₂), -3.11 (s, 18H, COT- $[\text{Si}\{\text{CH}(\text{CH}_3)_2\}_3]_2$), -0.53 (s, 6H, COT- $[\text{Si}\{\text{CH}(\text{CH}_3)_2\}_3]_2$), 30.81 (br s, $\Delta\nu_{1/2} = 314.93$ Hz, 2H, COT).

[U(η -C₈H₆{SiMe₃-1,4₂})(η -Cp^{Me₄TMS})]₂(μ - η^1 - η^1 -¹³C₂O₂) (14). A 50 mg portion of $[\text{U}(\eta\text{-C}_8\text{H}_6\{\text{SiMe}_3\text{-1,4}_2\})(\eta\text{-Cp}^{\text{Me}_4\text{TMS}})]$ (0.074 mmol) was dissolved in 0.5–0.7 mL of *d*₈-toluene in a 50 mL ampule equipped with a Young valve which was attached to the Toepler line, and the solution was cooled to -78°C and then degassed by evacuating the headspace at this temperature. ¹³CO (3 mol equiv) was transferred, and the reaction mixture was warmed to room temperature overnight, upon which time it adopted a red coloration with the formation of a small amount of red precipitate. The ¹H NMR of this crude solution was >95% pure (¹³C{¹H} NMR and ²⁹Si{¹H} NMR showed only one species in solution). Volatiles were removed under vacuum, and the red residue was washed with 3 × 3 mL of *n*-pentane at room temperature, filtered, and dried to yield 45 mg of the title compound in over >95% purity as judged by ¹H NMR spectroscopy. This residue was redissolved in the minimum amount of toluene/THF (1–2 mL, 1:1), and the solution was allowed to slowly evaporate over 2 days at room temperature in the glovebox, upon which time red crystals started forming. The solution was placed cooled to -35°C to complete crystallization and afford the title compound as red needles. Yield: 35 mg (81.5%). ¹H NMR (δ C_6D_6):

-53.55 (s, 4H, COT), -31.86 (s, 4H, COT), -12.06 (s, 36H, COT- $\{\text{Si}(\text{CH}_3)_3\}_2$), -5.01 (s, 12H, CH₃), -0.33 (s, 18H, Cp^{Me₄}-Si(CH₃)₃), 2.39 (s, 12H, CH₃), 50.64 (s, 4H, COT); ¹³C{¹H} NMR (δ C_7D_8): 287.17 ($[\text{U}]^{13}\text{C}_2\text{O}_2[\text{U}]$). ²⁹Si{¹H} NMR (δ C_7D_8): -143.17 and -108.33 (two singlets, COT- $\{\text{Si}(\text{CH}_3)_3\}_2$ and Cp^{Me₄}-Si(CH₃)₃). EI-MS: 1416 (M), 1268 (M – 2TMS), 1168 (M – TMS – Cp^{Me₄TMS} + F), 698 ($[\text{UCOT}^{\text{tms}2}\text{Cp}^{\text{Me}_4\text{TMS}}] + \text{F}$), 679 ($[\text{UCOT}^{\text{tms}2}\text{Cp}^{\text{Me}_4\text{TMS}}]$), 575 ($[\text{UCOT}^{\text{tms}2}\text{Cp}^{\text{Me}_4\text{TMS}}] - 2\text{TMS}$), 432 ($[\text{UCOT}^{\text{tms}2}] - \text{TMS} + \text{F}$), 248 ($\text{COT}^{\text{tms}2}$), 73 (TMS). Anal. Calcd for C₅₄H₉₀O₂Si₆U₂: C, 45.88; H, 6.40. Found: C, 45.51; H, 6.10.

Reaction of [U(η -C₈H₆{SiMe₃-1,4₂})(η -Cp^{Me₄TMS})] (9) with 1.5 bar of CO. A Young NMR tube was charged in the glovebox with 16 mg of 9 (0.023 mmol) that was dissolved in 0.5 mL of C_7D_8 . The brown solution was freeze–thaw degassed and the tube pressurized at either -78°C or room temperature with 1.5 bar (10 equiv) of CO. The ¹H NMR spectra showed only 14 as the major species (>90%).

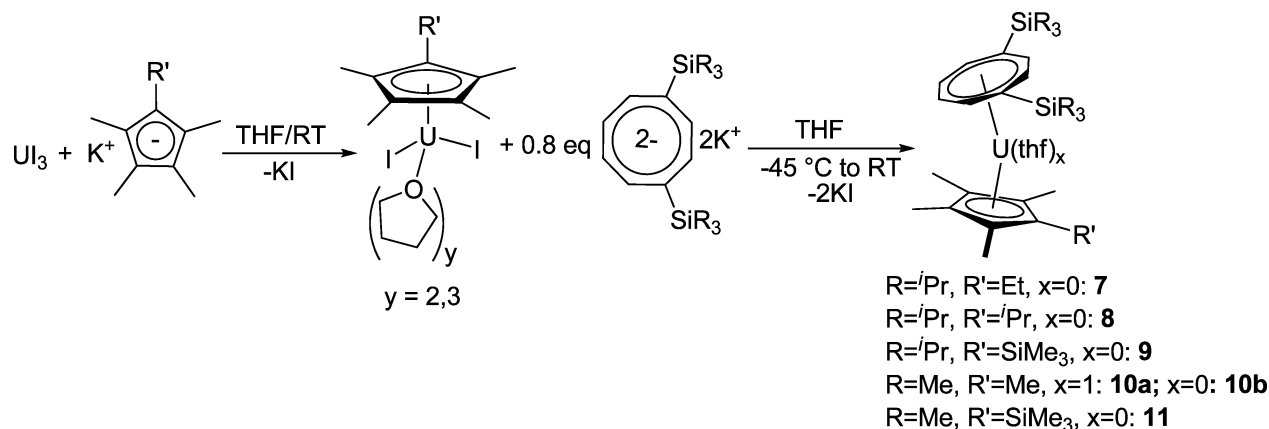
[U(η -C₈H₆{SiMe₃-1,4₂})(η -Cp^{*})]₂(μ - η^2 - η^2 -C₄O₄) (15). In a typical procedure 250 mg of $[\text{UCOT}^{\text{tms}2}\text{Cp}^*(\text{THF})]$ (0.36 mmol) was placed in a thick-walled ampule equipped with a greaseless stopcock and dissolved in approximately 5 mL of Et₂O. The solution was degassed by two freeze–thaw cycles, cooled to -78°C , pressurized with 1.5 bar of CO (10 equiv), and warmed to room temperature overnight. Volatiles were removed under vacuum, the red residue was extracted with toluene (approximately 10 mL), and the extract was filtered via cannula and cooled to -35°C to yield the title compound as large red blocks. Yield: 68 mg (28%). ¹H NMR (δ C_7D_8 , 30 $^\circ\text{C}$): -92.65 (s, 4H, COT), -82.78 (s, 4H, COT), -11.43 (br s, $\Delta\nu_{1/2} = 53.91$ Hz, 36H, COT-Si(CH₃)₃), 7.75 (s, 30H, Cp-(CH₃)₅), 56.65 (s, 4H, COT). ¹³C{¹H} NMR (δ C_7D_8 , 30 $^\circ\text{C}$): -127.07 (s, $\Delta\nu_{1/2} = 196.5$ Hz, $[\text{U}]^{13}\text{C}_4\text{O}_4[\text{U}]$). ²⁹Si{¹H} NMR (δ C_7D_8 , 30 $^\circ\text{C}$): -90.09 (s, COT- $\{\text{Si}(\text{CH}_3)_3\}_2$). ¹H NMR (δ C_7D_8 , -40°C): -134.15 (s, 2H, COT), -127.88 (s, 2H, COT), -112.22 (s, 4H, COT), -17.46 (s, 14H, COT-Si(CH₃)₃), -13.78 (s, 22H, COT-Si(CH₃)₃), -8.78 and -9.35 (2 singlets, 30H, Cp-(CH₃)₅), 78.45 (s, 2H, COT), 82.29 (s, 2H, COT). ¹³C{¹H} NMR (δ C_7D_8 , -40°C): -233.36 (br s, $\Delta\nu_{1/2} = 313.01$ Hz), -264.33 (br s, $\Delta\nu_{1/2} = 296.96$ Hz). ¹H NMR (δ C_7D_8 , 80 $^\circ\text{C}$): -69.62 (s, 4H, COT), -64.83 (s, 4H, COT), -8.98 (s, 36H, COT-Si(CH₃)₃), 6.85 (s, 30H, Cp-(CH₃)₅), 42.46 (s, 4H, COT). ¹³C{¹H} NMR (δ C_7D_8 , 80 $^\circ\text{C}$): -53.96 (s, $\Delta\nu_{1/2} = 89.12$ Hz, $[\text{U}]^{13}\text{C}_4\text{O}_4[\text{U}]$). EI-MS: 1359 (M), 1224 (M – Cp^{*}), 640 ($[\text{UCOT}^{\text{tms}2}\text{Cp}^*] + \text{F}$), 621 ($[\text{UCOT}^{\text{tms}2}\text{Cp}^*]$), 505 ($[\text{UCOT}^{\text{tms}2}] + \text{F}$), 392 (Cp^{*} + F), 248 ($\text{COT}^{\text{tms}2}$). Anal. Calcd for C₅₂H₇₈O₄Si₄U₂: C, 46.07; H, 5.80. Found: C, 46.03; H, 5.90.

¹³C-enriched 15 can be isolated in the same way as above using ¹³CO.

[U(η -C₈H₆{SiⁱPr₃-1,4₂})(η -Cp^{Me₄H})]Cl (16). To an *n*-pentane solution (15 mL) of 5 (200 mg, 0.24 mmol) was added 1.5 equiv of PhCH₂Cl in the glovebox, and the resulting red solution was shaken and allowed to react for 5 min. Volatiles were removed under vacuum, and the product was obtained as a glassy red solid by sublimation at $180\text{--}200^\circ\text{C}/10^{-6}$ mbar over 18 h. Yield: 128 mg (67%). ¹H NMR (δ C_6D_6 , 20 $^\circ\text{C}$): -108.1 (br s, 2H, COT), -88.3 (br s, 2H, COT), -9.8 (br s, 18H, COT- $[\text{Si}\{\text{CH}(\text{CH}_3)_2\}_3]_2$), -8.52 (br s, 18H, COT- $[\text{Si}\{\text{CH}(\text{CH}_3)_2\}_3]_2$), -7.78 (br s, 6H, COT- $[\text{Si}\{\text{CH}(\text{CH}_3)_2\}_3]_2$), 1.2 (br s, 1H, CpMe₄H), 2.5 (br s, 6H, Cp(CH₃)₄H), 16.8 (br s, 6H, Cp(CH₃)₄H), 20.5 (br s, 2H, COT). EI-MS: 811 (M), 768 (M – ¹Pr). Anal. Calcd for C₃₅H₆₁Cl₁Si₂U: C, 51.78; H, 7.52. Found: C, 51.67; H, 7.69.

Synthesis of ¹³C₄O₄(SiMe₃)₂ (17). To a solution of ¹³C-squarate enriched 5 (12 mg, 0.0072 mmol) in *d*₈-THF (0.5–0.7 mL) in a Young NMR tube in the glovebox was added 2.5 equiv of SiMe₃Cl (2.30 μL , 0.018 mmol) at room temperature. The solution was shaken and allowed to react for 5 min. Volatiles were removed under vacuum, and the red solids were extracted with *n*-pentane, giving 19 and leaving ¹³C₄O₄(SiMe₃)₂ as a pale yellow solid. Yield: quantitative. ¹H NMR (δ $\text{C}_4\text{D}_8\text{O}$, 20 $^\circ\text{C}$): 0.4 (s, 18H, ¹³C₄O₄(SiMe₃)₂). ¹³C{¹H} NMR (δ $\text{C}_4\text{D}_8\text{O}$, 20 $^\circ\text{C}$): see the Results and Discussion.

X-ray Crystallographic Studies. All data sets were collected on a Bruker-Nonius Kappa CCD area detector diffractometer with a sealed-tube source (Mo K α) and an Oxford Cryosystems low-temperature

Scheme 2. Synthesis of U(III) Mixed-Sandwich Complexes with $[\text{U}(\eta\text{-C}_8\text{H}_6\{\text{SiR}_3\text{-1,4}\}_2)(\eta\text{-Cp}^{\text{Me4R'}})(\text{THF})_x]$ 

device, operating in ω scanning mode with ψ and ω scans to fill the Ewald sphere. The programs used for control and integration were Collect,²⁵ Scalepack, and Denzo.²⁶ Absorption corrections were based on equivalent reflections using SADABS.²⁷ The crystals were mounted on a glass fiber with silicon grease, from dried vacuum oil kept over 4 Å in a MBraun glovebox under Ar. All solutions and refinements were performed using the WinGX package²⁸ and all software packages within. All non-hydrogen atoms were refined using anisotropic thermal parameters, and hydrogens were added using a riding model. Crystal structure and refinement data are given in Tables S1 and S2 of the Supporting Information. In **15** there is a disorder in the Cp* Me hydrogen atoms which was not treated with any constraints and split atoms were refined freely. Attempts to refine the non positive definite atom in **10b** using the ISOR command with a restraint as low as 0.01 resulted in it remaining a non positive definite atom. Investigation of the disorder in one of the TMS groups in **9** was not identified by ShelX, and application of the SQUEEZE routine to the model made the statistical factors of the model worse and the refinement failed to converge.

RESULTS AND DISCUSSION

Synthesis of U(III) Mixed-Sandwich Complexes. Since the extent of the reductive coupling of CO has been established to be affected by the steric environment around the metal center (vide supra), we decided to synthesize a range of new U(III) mixed-sandwich complexes $[\text{U}(\eta\text{-C}_8\text{H}_6\{\text{SiR}_3\text{-1,4}\}_2)(\eta\text{-Cp}^{\text{Me4R'}})(\text{THF})_x]$, varying the size of both R and R' in the latter (compounds **7–11** in Scheme 2). The general synthetic route shown in Scheme 2 results in moderate yields of the target compounds due to a competing disproportionation pathway that leads to the formation of the U(IV) uranocene complexes $[\text{U}(\eta\text{-C}_8\text{H}_6\{\text{SiR}_3\text{-1,4}\}_2)]$.²⁹ The first step in the synthesis is the formation of $[\text{U}(\eta\text{-Cp}^{\text{Me4R'}})\text{I}_2(\text{THF})_y]$, which is not isolated (see the Experimental Section) but used directly in the subsequent reaction with 0.8–0.9 mol equiv of $\text{K}_2[\text{C}_8\text{H}_6\{\text{SiR}_3\text{-1,4}\}_2]$ to furnish the title compounds. We have found that the use of this stoichiometry is crucial, as it inhibits the formation of the aforementioned uranocenes. In an effort to improve the yield of $[\text{U}(\eta\text{-C}_8\text{H}_6\{\text{SiMe}_3\text{-1,4}\}_2)(\eta\text{-Cp}^*)(\text{THF})]$ (**10a**), the isolated precursor $[\text{U}(\eta\text{-Cp}^*)\text{I}_2(\text{THF})_3]$ was reacted in a similar manner with $\text{K}_2[\text{C}_8\text{H}_6\{\text{SiMe}_3\text{-1,4}\}_2]$, but unfortunately this only resulted in a marginal increase (ca. 2%) in yield of the isolated complex after workup (see the Experimental Section).

Complexes **7–11** were fully characterized by spectroscopic and analytical methods. Their ^1H NMR spectra consist of paramagnetically shifted peaks in the region between -150 and

$+35$ ppm and are consistent with the formulations assigned. The $^{29}\text{Si}\{^1\text{H}\}$ NMR spectra of the compounds display the expected number of resonances, except in the case of **11**, where the resonance of the $[\text{Cp}^{\text{Me4}}\text{-SiMe}_3]^-$ ligand could not be located. Their mass spectra (EI mode) show the parent ion $(\text{M})^+$ as well as the fragment $(\text{M} + \text{F})^+$, and their isotopic distributions agree with the calculated isotopic envelopes. The origin of the $(\text{M} + \text{F})^+$ ion is undoubtedly due to the presence of traces of $\text{N}(\text{CF}_2\text{CF}_3)_3$ used for the calibration of the mass spectrometer and is to an extent expected due to the fluorophilic nature of uranium complexes.³⁰ Unfortunately, complexes **10a,b** and **11** are thermally unstable and decompose readily even in the solid state, and therefore reliable elemental analyses for these compounds could not be obtained. The proposed formulations of the complexes **7–9** were further confirmed by single-crystal X-ray crystallographic studies (Figure 3 and Table 1). Although complex **10a** crystallizes readily from *n*-pentane, single crystals suitable for an X-ray diffraction study could not be obtained, and therefore a molecular structure is not available. However, we were able to crystallize in good yields its desolvated derivative $[\text{U}(\eta\text{-C}_8\text{H}_6\{\text{SiMe}_3\text{-1,4}\}_2)(\eta\text{-Cp}^*)(\text{THF})]$ (**10b**), by exposure of complex **10a** to high vacuum (10^{-6} mbar) at $50\text{--}70$ °C. The molecular structure of **10b** is also presented in Figure 3. It is worth noting that, upon desolvation, the $^{29}\text{Si}\{^1\text{H}\}$ NMR signal for **10b** shifted downfield to -145.26 ppm from -176.25 ppm in **10a**, possibly due to the loss of the extra electron density provided by the THF coordination to the oxophilic U(III) center.

All four complexes display the expected bent-sandwich structure. It is worth noting that an increase of the steric hindrance of the R' substituent of the Cp ligand inhibits the coordination of THF in **7–9** as isolated from THF-containing reaction mixtures, in contrast to the case for $[\text{U}(\eta\text{-C}_8\text{H}_6\{\text{Si}^i\text{Pr}_3\text{-1,4}\}_2)(\eta\text{-Cp}^*)(\text{THF})]$ (**1**). The $\text{COT}_{\text{centroid}}\text{--U}$ bond distance in **10b** and **7** are the same within the esds but longer than those found in complexes **8** and **9**. On the other hand, all the $\text{Cp}_{\text{centroid}}\text{--U}$ bond distances are the same within the esds. The $\text{COT}_{\text{centroid}}\text{--U--Cp}_{\text{centroid}}$ bond angle increases with overall bulk around the metal center (**10b** vs **7–9**), while a small decrease in this angle is observed in the case of **8** and **9**, in comparison to **7**, presumably in order to release some of the steric strain. It is worth noticing that the Et group in **7** is pointing away from the Si^iPr_3 substituents of the COT ligand, while in the case of **8** and **9** the bulkier groups are orientated toward them.

In the case of complex **11**, the crystals were heavily twinned and, despite repeated efforts, a fully refined model of the

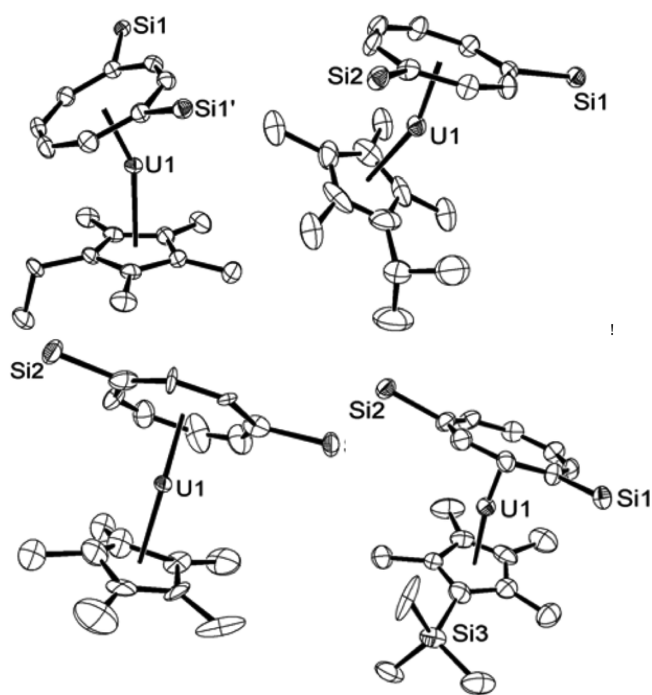


Figure 3. From top left clockwise, ORTEP drawings (50% probability ellipsoids) of the molecular structures of **7–9** and **10b** (alkyl groups on the silyl substituents of the $[\eta\text{-C}_8\text{H}_6\{\text{SiR}_3\text{-1,4}\}_2]^{2-}$ ligand and hydrogen atoms are omitted for clarity). U–COT_{centroid}, U–Cp_{centroid} distances (Å) and COT_{centroid}–U–Cp_{centroid} angles (deg) are given in Table 1.

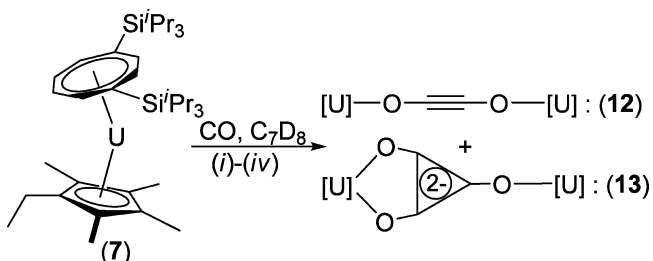
Table 1. Comparison of the U–COT_{centroid} and U–Cp_{centroid} Distances (Å) and COT_{centroid}–U–Cp_{centroid} Angles (deg) in complexes **7–9** and **10b**

complex	CO _{centroid} –U (Å)	Cp _{centroid} –U (Å)	COT _{centroid} –U–Cp _{centroid} (deg)
$[\text{U}(\eta\text{-C}_8\text{H}_6\{\text{Si}^i\text{Pr}_3\text{-1,4}\}_2)(\eta\text{-Cp}^{\text{Me4Et}})]$ (7)	1.920(10)	2.460(10)	155.6(4)
$[\text{U}(\eta\text{-C}_8\text{H}_6\{\text{Si}^i\text{Pr}_3\text{-1,4}\}_2)(\eta\text{-Cp}^{\text{Me4Et}})]$ (8)	1.910(11)	2.560(11)	153.0(3)
$[\text{U}(\eta\text{-C}_8\text{H}_6\{\text{Si}^i\text{Pr}_3\text{-1,4}\}_2)(\eta\text{-Cp}^{\text{Me4TMS}})]$ (9)	1.903(9)	2.450(10)	153.8(3)
$[\text{U}(\eta\text{-C}_8\text{H}_6\{\text{SiMe}_3\text{-1,4}\}_2)(\eta\text{-Cp}^*)]$ (10b)	1.971(15)	2.440(15)	139.1(6)

diffraction experiment could not be obtained. Despite this fact, the initial solution and partially refined model (R1 = 4.8%) is in agreement with the proposed formulation (see the Supporting Information).

Reactivity of **7–11 with CO.** Addition of 2 or 3 equiv of ^{13}CO to a C_7D_8 solution of **7** at -78°C followed by slow warming to room temperature results in the formation of a reaction mixture that consists of two major species by ^1H NMR and $^{13}\text{C}\{^1\text{H}\}$ NMR. More specifically, the $^{13}\text{C}\{^1\text{H}\}$ NMR spectrum shows two new major peaks at 315.46 and 224.35 ppm in a relative ratio of 9:1, respectively. The ^1H NMR spectrum was also informative, as it clearly shows two sets of peaks for the diastereotopic methyl groups of the Si^iPr_3 groups of the substituted cyclooctatetraenyl ligand in the same region of the spectrum also in a relative ratio of 9:1. On the basis of the almost identical $^{13}\text{C}\{^1\text{H}\}$ NMR chemical shifts of the aforementioned species in comparison with those reported for the U(IV) dimers **3**¹² and **4**¹⁰ (Scheme 1), we tentatively assigned the two components of the reaction mixture as $[\text{U}(\eta\text{-C}_8\text{H}_6\{\text{Si}^i\text{Pr}_3\text{-1,4}\}_2)(\eta\text{-Cp}^{\text{Me4Et}})]_2(\mu\text{-}\eta^1\text{:}\eta^1\text{-C}_2\text{O}_2)$ (**12**) and $[\text{U}(\eta\text{-C}_8\text{H}_6\{\text{Si}^i\text{Pr}_3\text{-1,4}\}_2)(\eta\text{-Cp}^{\text{Me4Et}})]_2(\mu\text{-}\eta^1\text{:}\eta^2\text{-C}_3\text{O}_3)$ (**13**), corresponding to the $^{13}\text{C}\{^1\text{H}\}$ NMR chemical shifts of 315.46 and 224.35 ppm, respectively (Scheme 3).

Scheme 3. Reactivity of **7** toward CO^a



^aReaction conditions: (i) 2 or 3 equiv of ^{13}CO , -78°C to room temperature, **12**:**13** = 9:1; (ii) 5.4 equiv of ^{13}CO , room temperature, **12**:**13** = 5:1; (iii) 1.5 bar (10 equiv) of CO , -78°C to room temperature, **12**:**13** = 5:1; (iv): 1.5 bar of CO (10 equiv), room temperature, **12**:**13** = 3:1.

Furthermore, a mass spectrum of the reaction mixture after removal of the volatiles showed the parent ions of these two dimers at 1666 and 1695 Da, respectively. The two complexes can be separated by repeated fractional crystallizations from *n*-pentane at low temperatures (-20°C), and indeed the identity of **12** was confirmed by X-ray crystallography and is shown in Figure 4.

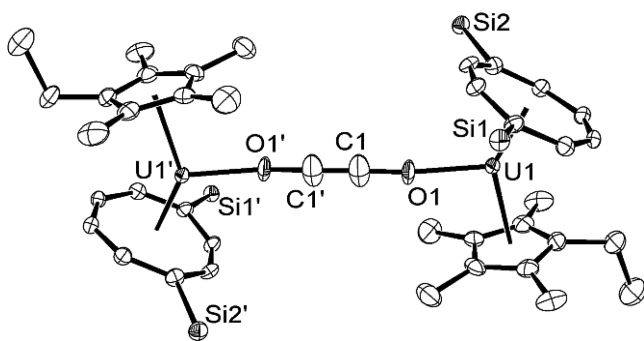


Figure 4. ORTEP drawing (50% probability ellipsoids) of the molecular structure of **12** (isopropyl groups and hydrogen atoms omitted for clarity). Selected bond lengths (Å) and angles (deg): U1–O1 = 2.155(3), O1–C1 = 1.262(6), C1–C1' = 1.215(10), U1–COT_{centroid} = 1.926(7), U1–Cp_{centroid} = 2.469(7); U1–O1–C1 = 173.7(4), O1–C1–C1' = 176.9(10), COT_{centroid}–U1–Cp_{centroid} = 139.8(3).

The C–C bond distance in the C_2O_2 moiety is 1.215(10) Å, is similar within the esds with that reported for $[\text{U}(\eta\text{-C}_8\text{H}_6\{\text{Si}^i\text{Pr}_3\text{-1,4}\}_2)(\eta\text{-Cp}^*)]_2(\mu\text{-}\eta^1\text{:}\eta^1\text{-C}_2\text{O}_2)$ (**3**; 1.117(12) Å),¹² and is consistent with a C–C triple bond. The C–O–U angle of $173.7(4)^\circ$ in **12** is slightly less than the almost linear angle of $178.3(7)^\circ$ found in **3**. It is also worth noting that the ethyl group of the $[\text{Cp}^{\text{Me4Et}}]$ ligand is pointing away from the C_2O_2 moiety, probably to reduce steric strain. Other spectroscopic data are in agreement with the proposed formula and the molecular structure of **12** discussed above. In more detail, the ^1H NMR spectrum confirms a C_{2h} -symmetric structure with the resonances spanning a range from -55 to $+60$ ppm. The $^{13}\text{C}\{^1\text{H}\}$ NMR spectrum consists of only one

major peak at 315.46 ppm in the ^{13}C -enriched sample, while the $^{29}\text{Si}\{^1\text{H}\}$ NMR spectrum shows one peak at -112.54 ppm, shifted downfield from -136.65 ppm in the starting U(III) complex **7**. Unfortunately, the second product **13** has eluded isolation and crystallographic characterization thus far.

The addition of CO (0.85 bar, 5.4 mol equiv) was also performed at room temperature in order to probe whether the steric environment is the determining factor and that the observed product distribution is not a result of the reaction being under kinetic control, as proposed by the theoretical calculations.¹³ In this case again the same products were formed, but the ratio **12**:**13** was now 5:1. This may seem to contradict the proposed reaction pathway,¹³ but since both the deltate and ynediolate are observed, this means that increasing the steric bulk around the uranium center probably inhibits the formation of the proposed side-on $[\text{U}(\mu\text{-}\eta\text{-CO})[\text{U}]$ intermediate responsible for the formation of the deltate dimer. In order to probe this further, a Young NMR tube was pressurized with 1.5 bar (10 equiv) of CO at room temperature, and again complex **12** was found to be the major product with the product ratio **12**:**13** being approximately 3:1 (by integration of the ^1H NMR signals corresponding to the diastereotopic Si^{ipr3} methyls). Finally the addition of a large overpressure of CO (1.5 bar, 10 equiv) was performed at -78°C followed by slow warming to room temperature to reveal an approximately 5:1 mixture of **12** and **13**. This effect of pressure is in agreement with the theoretically derived mechanism, which predicts that in the presence of a large excess of CO the formation of the deltate dimer is favored.¹³

Since the formation of deltate has been significantly inhibited by employing the Cp^{Me4Et} ligand, the more sterically encumbered complex $[\text{U}(\eta\text{-C}_8\text{H}_6\{\text{Si}^{\text{iPr3}}\text{Pr}_3\text{-1,4}\}_2)(\eta\text{-Cp}^{\text{Me4iPr}})]$ (**8**) was reacted with 2–3 equiv of ^{13}CO in a manner similar to that above. In this case no apparent reaction was observed, even when the reaction mixture was left at room temperature overnight. The $^{13}\text{C}\{^1\text{H}\}$ NMR spectrum showed no peaks apart from unreacted ^{13}CO (185 ppm) and solvent signals; however, some of the peaks in the ^1H NMR spectrum were slightly shifted compared to those in the starting material (see the Experimental Section). On the basis of these observations we envisaged that, due to the increased steric hindrance around the metal center, the reductive coupling of CO does not proceed further than the coordination of CO to the U(III) center. We therefore decided to probe the reaction by in situ IR spectroscopy. Unfortunately, no characteristic peaks in the fingerprint region for coordinated CO were observed, even at room temperature. In order to determine whether the concentration of CO is important, an NMR sample of **8** in C_7D_8 in a Young tube was pressurized with 1.5 bar (10 equiv) of CO. Again no reaction was observed and the ^1H NMR spectrum showed peaks consistent with complex **8**, but with chemical shifts slightly different from those in an authentic sample of **8**.

On the basis of the discussion above, it came as no surprise that the complex $[\text{U}(\eta\text{-C}_8\text{H}_6\{\text{Si}^{\text{iPr3}}\text{Pr}_3\text{-1,4}\}_2)(\eta\text{-Cp}^{\text{Me4TMS}})]$ (**9**) shows no evidence for any reaction with CO, even at higher pressures (1.5–2.0 bar, 10–15 equiv) or elevated temperatures ($60\text{--}70^\circ\text{C}$).

Since the increased steric hindrance in complexes **8** and **9** clearly inhibits the reactivity of these complexes with CO, we decided to alter the steric environment of the U(III) metal center by employing the less bulky $[\eta\text{-C}_8\text{H}_6\{\text{SiMe}_3\text{-1,4}\}_2]^{2-}$ ligand. Indeed, the reaction of $[\text{U}(\eta\text{-C}_8\text{H}_6\{\text{SiMe}_3\text{-1,4}\}_2)(\eta\text{-Cp}^{\text{Me4TMS}})]$ (**11**) with an excess of ^{13}CO (2–5 mol equiv) at -78°C or room temperature yielded a very clean reaction mixture, as judged by ^1H NMR and $^{13}\text{C}\{^1\text{H}\}$ NMR spectroscopy. The latter consists of only one new, sharp peak at 287.17 ppm. Furthermore, the ^1H NMR spectrum is consistent with a symmetrical structure, while the $^{29}\text{Si}\{^1\text{H}\}$ NMR spectrum displays two signals at -143.17 and -108.33 ppm for the $-\text{SiMe}_3$ substituents on the cyclooctatetraenyl and cyclopentadienyl ligands. Finally, the mass spectrum showed a molecular ion at 1413 D_a which is consistent with the formulation $[\text{U}(\eta\text{-C}_8\text{H}_6\{\text{SiMe}_3\text{-1,4}\}_2)(\eta\text{-Cp}^{\text{Me4TMS}})]_2(\mu\text{-}\eta^1\text{-}\eta^1\text{-}^{13}\text{C}_2\text{O}_2)$ (**14**). A single-crystal X-ray crystallographic study confirmed this, and Figure 5 shows the ORTEP diagram of the molecular structure of **14**.

Figure 5. ORTEP drawing (50% probability ellipsoids) of the molecular structure of **14** (methyl groups of the COT silyl substituents and hydrogen atoms omitted for clarity). Selected bond lengths (Å) and angles (deg): C1–C1' = 1.176(10), C1–O1 = 1.307(5), U1–O1 = 2.159(3), U1–COT_{centroid} = 1.910(9), U–Cp_{centroid} = 2.462(9); U1–O1–C1 = 149.7(3), O1–C1–C1' = 176.4(7), COT_{centroid}–U1–Cp_{centroid} = 139.7(3).

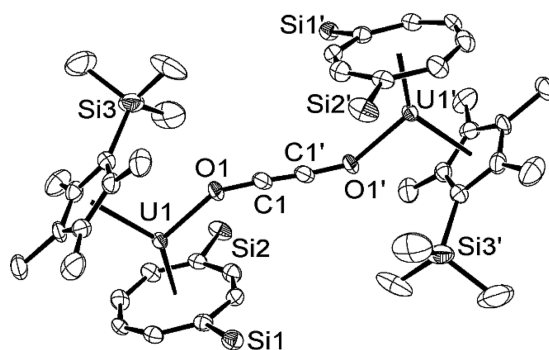


Figure 5. ORTEP drawing (50% probability ellipsoids) of the molecular structure of **14** (methyl groups of the COT silyl substituents and hydrogen atoms omitted for clarity). Selected bond lengths (Å) and angles (deg): C1–C1' = 1.176(10), C1–O1 = 1.307(5), U1–O1 = 2.159(3), U1–COT_{centroid} = 1.910(9), U–Cp_{centroid} = 2.462(9); U1–O1–C1 = 149.7(3), O1–C1–C1' = 176.4(7), COT_{centroid}–U1–Cp_{centroid} = 139.7(3).

Again the C–C bond distance of 1.176(10) Å in the C_2O_2 moiety is consistent with a triple bond and is similar, within the esds, with those found in both **3**¹² and **12**. The U–O distances in complexes **12**, **14**, and **3**¹² are identical within the esds. Unlike **12**, the bulky TMS group of the $[\text{Cp}^{\text{Me4TMS}}]$ ligand is pointing inward to the C_2O_2 moiety. This results in an acute C–O–U angle of $149.7(3)^\circ$, deviating from the angle of $173.7(4)^\circ$ found in **12** or the almost linear angle of $178.3(7)^\circ$ found in **3**.¹² This deviation is also reflected in the corresponding torsion angles of $5.34(10)$ and $100.88(5)^\circ$ for **14** and **12**, respectively. The C–O bond distance in **14** is the same within esds with that reported for **3** but slightly longer (0.045 Å) than that found in **12**. The reason for this is unclear, but a plausible explanation could be found in the deviation from linearity of the C–O–U angle, imposed by the bulky SiMe_3 group of the $[\text{Cp}^{\text{Me4TMS}}]$ ligand.

The formation of **14** as the sole product of the reaction of **11** with CO is also independent of the CO overpressure (up to 1.5 bar), unlike in the case of **7**. The release of the steric constraints imposed by the use of the $[\eta\text{-C}_8\text{H}_6\{\text{Si}^{\text{iPr3}}\text{Pr}_3\text{-1,4}\}_2]^{2-}$ ligand, combined with the increased steric hindrance of the $[\eta\text{-Cp}^{\text{Me4TMS}}]^-$ substituent, on one hand allows the reaction with CO while on the other stops the reductive coupling of more than two CO molecules. One explanation could be due to the orientation of the bulky $-\text{SiMe}_3$ group in the $[\eta\text{-Cp}^{\text{Me4TMS}}]^-$ ligand towards the bridging ynediolate unit. This could in principle inhibit the formation of the $[\text{U}(\mu\text{-}\eta^2\text{-CO})[\text{U}]$ dimer,

predicted by theoretical calculations to be the first step in the formation of the deltate dimer.^{12,13}

The effect of the steric environment in the reductive coupling of CO was further demonstrated by the reaction of $[\text{U}(\eta\text{-C}_8\text{H}_6\{\text{SiMe}_3\text{-1,4}\}_2)(\eta\text{-Cp}^*)\text{THF}]$ (**10a**) with CO. Upon exposure of the latter to ^{13}CO (1.5–8 equiv) in C_7D_8 , a complex reaction mixture was obtained. $^{13}\text{C}\{^1\text{H}\}$ NMR spectroscopy confirmed the existence of more than one species, but for all stoichiometries of **10a**/ ^{13}CO used, a broad peak ($\Delta\nu_{1/2} = 196.5$ Hz) at -127.07 ppm was observed to be the major one. This $^{13}\text{C}\{^1\text{H}\}$ NMR chemical shift is in the same region as that reported (-111.4 ppm in $\text{C}_4\text{D}_8\text{O}$) for the squarate complex $[\text{U}(\eta\text{-C}_8\text{H}_6\{\text{SiPr}_3\text{-1,4}\}_2)(\eta\text{-Cp}^{\text{Me4H}})]_2(\mu\text{-}\eta^2\text{-}\eta^2\text{-}^{13}\text{C}_4\text{O}_4)$ (**5**).¹¹ Crystalline **15** was isolated from the reaction mixture by recrystallization from the minimum amount of toluene at -35 °C. The ^1H NMR spectrum of **15** consists of broad peaks at -92.65 , -82.78 , and 56.65 ppm, integrating for 4H, corresponding to the $[\eta\text{-C}_8\text{H}_6\{\text{SiMe}_3\text{-1,4}\}_2]^{2-}$ ligand protons, and two singlets at -11.43 ppm (broad, $\Delta\nu_{1/2} = 53.91$ Hz) and 7.75 ppm, integrating respectively for 36H and 30H, corresponding to the $-\text{Si}(\text{CH}_3)_3$ and $\text{Cp}(\text{CH}_3)_5$ protons, respectively. The $^{13}\text{C}\{^1\text{H}\}$ NMR spectrum showed one broad peak at -127.09 ppm, while the $^{29}\text{Si}\{^1\text{H}\}$ NMR spectrum consisted of only one peak at -90.09 ppm, shifted downfield from -176.25 ppm in **10a**. The mass spectrum of **15** showed a molecular ion at 1359 Da with an isotopic envelope consistent with the formulation $[\text{U}(\eta\text{-C}_8\text{H}_6\{\text{SiMe}_3\text{-1,4}\}_2)(\eta\text{-Cp}^*)]_2(\mu\text{-}\eta^2\text{-}\eta^2\text{-}^{13}\text{C}_4\text{O}_4)$. The identity of **15** was finally unambiguously confirmed by a single-crystal X-ray diffraction study, and its molecular structure is shown in Figure 6.

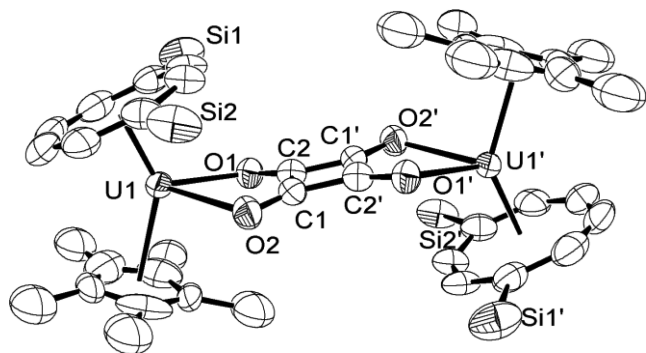


Figure 6. ORTEP drawing (50% probability ellipsoids) of the molecular structure of **15** (methyl groups of the COT silyl substituents and hydrogen atoms omitted for clarity). Selected bond lengths (Å) and angles (deg): C2–O1 = 1.253(8), U1–O1 = 2.485(5), U1–O2 = 2.490(5), C2–C1' = 1.455(10), C1–C2 = 1.456(10), C1–C2' = 1.455(10), C1'–C2' = 1.455(10), U1–COT_{centroid} = 1.945(5), U–Cp_{centroid} = 2.456(8); COT_{centroid}–U1–Cp_{centroid} = 140.8(3), O1–U1–O2 = 73.87(16), O1–C2–C1' = 142.1(7), O1–C2–C1 = 127.7(7), O2–C1–C2 = 127.5(7), C1'–C2–C1 = 90.2 (6), O2–C1–C2' = 142.7(7).

The U–O bond distances of 2.485(5) and 2.490(5) Å in **15** are the same within the esds as those reported for **5**, as are the metrical parameters for the squarate unit, and so will not be discussed further.¹¹

Functionalization of Uranium-Bound Oxocarbons. Liddle et al. have reported the extrusion of the $\text{C}_2\text{O}_2^{2-}$ moiety from $[\{\text{U}(\text{Tren}^{\text{DMSB}})\}_2(\mu\text{-}\eta^1\text{-}\eta^1\text{-}^{13}\text{C}_2\text{O}_2)]$ ($\text{Tren}^{\text{DMSB}} = \text{N}(\text{CH}_2\text{CH}_2\text{NSiMe}_2\text{But})_3$) with $\text{SiMe}_2\text{R-I}$ ($\text{R} = \text{Me}, \text{Ph}$) to produce $[\text{U}(\text{Tren}^{\text{DMSB}})]$ and $\text{SiMe}_2\text{ROC}\equiv\text{COSiMe}_2\text{R}$; aque-

ous workup of the latter gives a mixture of 3,4-bis-($\text{Me}_2\text{Rsilyloxy}$)furan-2(*SH*)-ones and 3,4-bis-($\text{Me}_2\text{Rsilyloxy}$)-furan-2-ols.¹⁵

When $[\text{U}(\eta\text{-C}_8\text{H}_6\{\text{Si}^i\text{Pr}_3\text{-1,4}\}_2)(\eta\text{-Cp}^{\text{Me4Et}})]_2(\mu\text{-}\eta^1\text{-}\eta^1\text{-}^{13}\text{C}_2\text{O}_2)$ (**12**) or $[\text{U}(\eta\text{-C}_8\text{H}_6\{\text{SiMe}_3\text{-1,4}\}_2)(\eta\text{-Cp}^{\text{Me4TMS}})]_2(\mu\text{-}\eta^1\text{-}\eta^1\text{-}^{13}\text{C}_2\text{O}_2)$ (**14**) was reacted with $\text{SiMe}_3\text{-I}$ in d_8 -toluene, the first produced an intractable reaction mixture while the latter failed to react even at elevated temperatures (70 °C), possibly due to the increased steric protection around the C_2O_2 moiety.

In order to try and expand the scope of possible CO functionalization, we turned our attention to $[\text{U}(\eta\text{-C}_8\text{H}_6\{\text{SiPr}_3\text{-1,4}\}_2)(\eta\text{-Cp}^{\text{Me4H}})]_2(\mu\text{-}\eta^2\text{-}\eta^2\text{-}^{13}\text{C}_4\text{O}_4)$ (**5**). **5** reacted cleanly with $\text{SiMe}_3\text{-Cl}$ in d_8 -THF (Scheme 4), as evidenced by the disappearance of the $^{13}\text{C}_4\text{O}_4$ peak at -111.4 ppm in the $^{13}\text{C}\{^1\text{H}\}$ NMR spectrum and its replacement by two complex multiplets centered at 195 and 188 ppm. The ^1H NMR spectrum showed the disappearance of resonances attributed to **5** and the appearance of a new set of resonances attributed to $[\text{U}(\eta\text{-C}_8\text{H}_6\{\text{SiPr}_3\text{-1,4}\}_2)(\eta\text{-Cp}^{\text{Me4H}})\text{Cl}]$ (**16**) (the identity of **16** was confirmed by its independent synthesis from $[\text{U}(\eta\text{-C}_8\text{H}_6\{\text{SiPr}_3\text{-1,4}\}_2)(\eta\text{-Cp}^{\text{Me4H}})(\text{THF})]$ (**2**) and PhCH_2Cl ; see the Experimental Section) and a new singlet at 0.04 ppm.

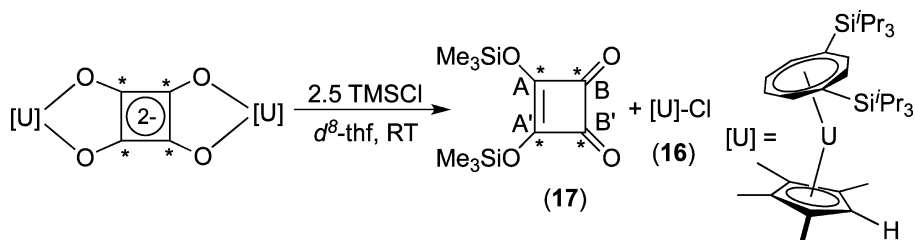
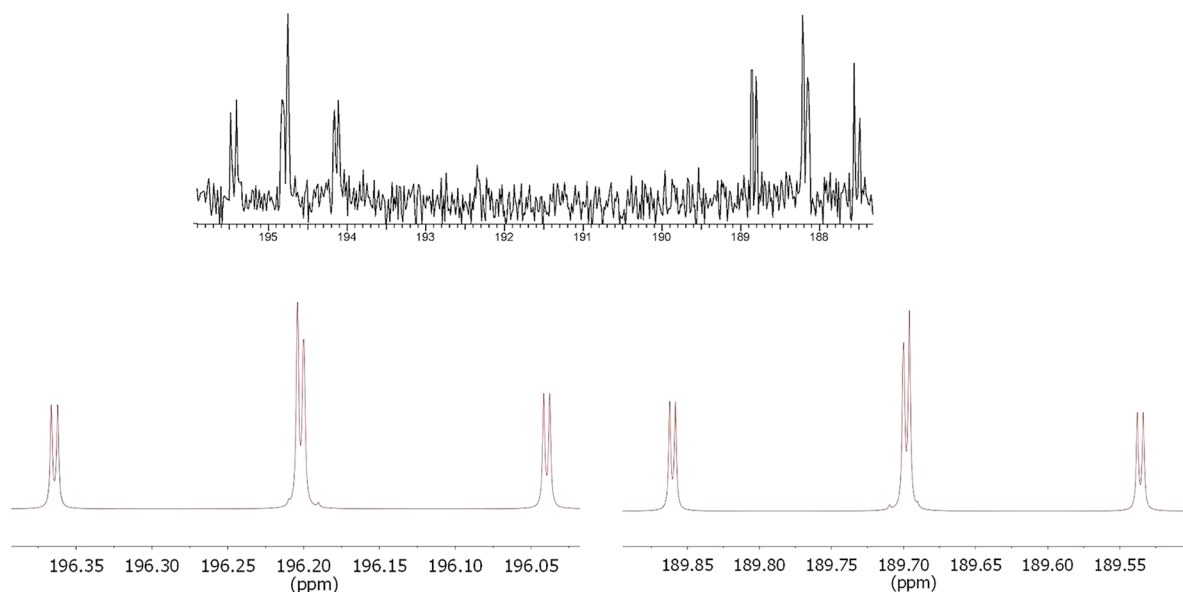
On closer inspection of the $^{13}\text{C}\{^1\text{H}\}$ NMR spectrum (Figure 7) a complex second-order splitting pattern is apparent, due to the AA'BB' spin system arising for $^{13}\text{C}_4\text{O}_4(\text{SiMe}_3)_2$ (**17**) (Scheme 4), which can be simulated with the following coupling constants: $J_{\text{AB}} = J_{\text{A'B'}} = 49.3$ Hz, $J_{\text{AB'}} = J_{\text{A'B}} = 48.1$ Hz, $J_{\text{AA'}} = 93.4$ Hz, $J_{\text{BB'}} = 90.6$ Hz (Figure 7).

To the best of our knowledge, this is the only example of a fully isotopically enriched four-membered carbocycle. Simple derivatives of squaric acid and the squarate dianion are currently used extensively in medicinal chemistry,³¹ bioconjugate chemistry,³² materials science,³³ photochemistry,³⁴ and organic synthesis.³⁵ They have also been investigated for their antitumor properties and as protein inhibitors.²⁰

Attempts to try and remove the deltate dianion from $[\text{U}(\eta\text{-C}_8\text{H}_6\{\text{SiPr}_3\text{-1,4}\}_2)(\eta\text{-Cp}^*)]_2(\mu\text{-}\eta^2\text{-}\eta^2\text{-}^{13}\text{C}_3\text{O}_3)$ (**2**) using a protocol similar to that for **5** were unfortunately fruitless, due to extensive decomposition leading to intractable mixtures.

CONCLUSION

In summary, we have demonstrated the effect of the steric environment around the uranium center in the reductive coupling of CO by complexes of the type $[\text{U}(\eta\text{-C}_8\text{H}_6\{\text{SiR}_3\text{-1,4}\}_2)(\eta\text{-Cp}^{\text{Me4R'}})]$. The reactivity is dominated by the “global” sterics around the uranium center, while selectivity is regulated by the steric bulk of the $\text{Cp}^{\text{Me4R'}}$ ligand. Hence, when the COT substituents are $^i\text{Pr}_3\text{Si}$, Cp^{Me4H} results in reductive tetramerization of CO to give the squarate complex, Cp^{Me5} reductively trimerizes CO to deltate, Cp^{Me4Et} gives a mixture of ynediolate (the result of reductive dimerization of CO) and deltate complexes, and use of $\text{Cp}^{\text{Me4iPr}}$ or $\text{Cp}^{\text{Me4SiMe3}}$ results in no reactivity toward CO. The use of the less sterically demanding SiMe_3 substituents on the COT ring in conjunction with the bulky $\text{Cp}^{\text{Me4SiMe3}}$ ligand results in completely selective formation of the ynediolate complex, even with a large excess of CO. The ability to isolate $^{13}\text{C}_4\text{O}_4(\text{SiMe}_3)_2$ (**17**) from **5** offers a novel route to ^{13}C -enriched carbocycles from ^{13}CO in an atom-efficient manner.

Scheme 4. Reactivity of **5** with SiMe_3Cl To Release $\text{C}_4\text{O}_4(\text{SiMe}_3)_2$ (**17**) and form **16**^a^aAsterisks denote ^{13}C -enriched carbons.Figure 7. Experimental (top) and simulated (lower) $^{13}\text{C}\{^1\text{H}\}$ NMR spectra of $^{13}\text{C}_4\text{O}_4(\text{TMS})_2$.

■ ASSOCIATED CONTENT

Supporting Information

Tables S1 and S2 and CIF files giving crystal structure and refinement data for **7–9**, **10b**, **12**, **14**, and **15** and a figure giving the not fully refined molecular structure of **11**. This material is available free of charge via the Internet at <http://pubs.acs.org>.

■ AUTHOR INFORMATION

Corresponding Author

*E-mail: f.g.cloke@sussex.ac.uk.

Notes

The authors declare no competing financial interest.

■ ACKNOWLEDGMENTS

We thank the ERC (N.T., F.G.N.C.) and EPSRC (O.T.S.) for financial support.

■ REFERENCES

- (1) (a) *Activation of Small Molecules: Organometallic and Binorganic Perspectives*; Tolman, W. B., Ed.; Wiley-VCH: Weinheim, Germany, 2006. (b) Stephan, D. W. *Dalton Trans.* **2009**, 3129. (c) Stephan, D. W. *Chem. Commun.* **2010**, 46, 8526. (d) Hazari, N. *Chem. Soc. Rev.* **2010**, 39, 4044. (e) Cavaliere, V. N.; Mendiola, D. J. *Chem. Sci.* **2012**, 3, 3356. (f) Mandal, S. W.; Roesky, H. W. *Acc. Chem. Res.* **2012**, 45, 298. (g) Yao, S.; Driess, M. *Acc. Chem. Res.* **2012**, 45, 276.
- (2) (a) Arnold, P. L. *Chem. Commun.* **2011**, 47, 9005. (b) Castro-Rodríguez, I.; Meyer, K. *Chem. Commun.* **2006**, 1353. (c) Lam, O. P.; Anthon, C.; Karsten, M. *Dalton Trans.* **2009**, 9677.
- (3) (a) Roussel, P.; Scott, P. J. *Am. Chem. Soc.* **1998**, 120, 1070. (b) Odom, A. L.; Arnold, P. L.; Cummins, C. C. *J. Am. Chem. Soc.* **1998**, 120, 5836. (c) Cloke, F. G. N.; Hitchcock, P. B. *J. Am. Chem. Soc.* **2002**, 124, 9352. (d) Cloke, F. G. N.; Green, J. C.; Kaltsoyannis, N. *Organometallics* **2004**, 23, 832.
- (4) Castro-Rodríguez, I.; Nakai, H.; Zakharov, L. N.; Rheingold, A. L.; Meyer, K. *Science* **2004**, 305, 1757.
- (5) Siladke, N. A.; Meihaus, K. R.; Ziller, J. W.; Fang, M.; Furche, F.; Long, J. R.; Evans, W. J. *J. Am. Chem. Soc.* **2012**, 134, 1243.
- (6) (a) Brennan, J. G.; Andersen, R. A.; Robbins, J. L. *J. Am. Chem. Soc.* **1986**, 108, 335. (b) Castro-Rodríguez, I.; Meyer, K. *J. Am. Chem. Soc.* **2005**, 127, 11242.
- (7) Ford, P. C. *Acc. Chem. Res.* **1981**, 14, 31 and references therein.
- (8) van Leeuwen, P. W. N. M. *Homogeneous Catalysis: Understanding the Art*; Kluwer Academic: Dordrecht, The Netherlands, 2003.
- (9) (a) Buchner, W. *Helv. Chim. Acta* **1963**, 46, 2111. (b) Gmelin, L. *Ann. Phys. Chem.* **1825**, 4, 31. (c) Lednor, P. W.; Versloot, P. C. *Chem. Commun.* **1983**, 285. (d) Silvestri, G.; Gambino, S.; Filardo, G.; Spadaro, G.; Palmisano, L. *Electrochim. Acta* **1978**, 23, 413. (e) Coluccia, S.; Garrone, E.; Guglielminotti, E.; Zecchina, A. *J. Chem. Soc., Faraday Trans. 1* **1981**, 77, 1063.
- (10) Summerscales, O. T.; Cloke, F. G. N.; Hitchcock, P. B.; Green, J. C.; Hazari, N. *Science* **2006**, 311, 829.
- (11) Summerscales, O. T.; Cloke, F. G. N.; Hitchcock, P. B.; Green, J. C.; Hazari, N. *J. Am. Chem. Soc.* **2006**, 128, 9602.
- (12) Frey, A. S.; Cloke, F. G. N.; Hitchcock, P. B.; Day, I. J.; Green, J. C.; Aitken, G. J. *Am. Chem. Soc.* **2008**, 130, 13816.
- (13) McKay, D.; Frey, A. S.; Green, J. C.; Cloke, F. G. N.; Maron, L. *Chem. Commun.* **2012**, 48, 4118.
- (14) Arnold, P. L.; Turner, Z. R.; Bellabarba, R. M.; Tooze, R. P. *Chem. Sci.* **2011**, 2, 77.

- (15) Gardner, B. M.; Stewart, J. C.; Davis, A. L.; McMaster, J.; Lewis, W.; Blake, A. J.; Liddle, S. T. *Proc. Natl. Acad. Sci. U.S.A.* **2012**, *109*, 9265.
- (16) Frey, A. S.; Cloke, F. G. N.; Coles, M. P.; Maron, L.; Davin, T. *Angew. Chem., Int. Ed.* **2011**, *50*, 6881.
- (17) Schumann, H.; Zietzke, K.; Erbstein, F.; Weimann, R. *J. Organomet. Chem.* **1996**, *520*, 265.
- (18) Clentsmith, G. K. B.; Cloke, F. G. N.; Francis, M. D.; Hanks, J. R.; Hitchcock, P. B.; Nixon, J. F. *J. Organomet. Chem.* **2008**, *693*, 2287.
- (19) Avens, L. R.; Burns, C. J.; Butcher, R. J.; Clark, D. L.; Gordon, J. C.; Schake, A. R.; Scott, B. L.; Watkin, J. G.; Zwick, B. D. *Organometallics* **2000**, *19*, 451.
- (20) Krutko, D. P.; Borzov, M. V.; Veksler, E. N. *Russ. Chem. Bull.* **2004**, *53*, 2182.
- (21) Burton, N. C.; Cloke, F. G. N.; Joseph, S. C. P.; Karamallakis, H.; Sameh, A. A. *J. Organomet. Chem.* **1993**, *462*, 39.
- (22) Schlosser, M.; Hartmann, J. *Angew. Chem., Int. Ed.* **1973**, *12*, 508.
- (23) Schumann, H.; Keitsch, M. R.; Winterfeld, J.; Mühle, S.; Molander, G. A. *J. Organomet. Chem.* **1998**, *559*, 181.
- (24) Evans, W. J.; Forrestal, K. J.; Ziller, J. W. *Polyhedron* **1998**, *17*, 4015.
- (25) Collect; Bruker-AXS BV, 1997–2004.
- (26) Otwinowski, Z.; Minor, W. SCALEPACK, DENZO. *Methods Enzymol.* **1997**, *276*, 307.
- (27) Sheldrick, G. M. SADABS V2008/1; University of Göttingen, Göttingen, Germany.
- (28) Farrugia, L. J. *J. Appl. Crystallogr.* **1999**, *32*, 83.
- (29) Schake, A. R.; Avens, L. R.; Burns, C. J.; Clark, D. L.; Sattelberger, A. P.; Smith, W. H. *Organometallics* **1993**, *12*, 1497.
- (30) Weydert, M.; Andersen, R. A.; Bergman, R. G. *J. Am. Chem. Soc.* **1993**, *115*, 8837.
- (31) Xie, J.; Comeau, A. B.; Seto, C. T. *Org. Lett.* **2004**, *6*, 83.
- (32) Aime, S.; Botta, M.; Grich, S. G.; Giovenzana, G.; Palnisana, G.; Sisti, M. *Bioconjugate Chem.* **1999**, *10*, 192.
- (33) Ajayaghosh, A.; Eldo, J. *Org. Lett.* **2001**, *3*, 2595.
- (34) Law, K. Y. *Chem. Rev.* **1993**, *93*, 449.
- (35) (a) Paquette, L. A.; Sturino, C. F.; Doussot, P. *J. Am. Chem. Soc.* **1996**, *118*, 9456. (b) Huffman, M. A.; Liebeskind, L. S. *J. Am. Chem. Soc.* **1993**, *115*, 4895. (c) Liebeskind, L. S. *Tetrahedron* **1989**, *45*, 3053. (d) Tomooka, C. S.; Liu, H.; Moore, H. W. *J. Org. Chem.* **1996**, *61*, 6009.